PHYSICAL REVIEW B **83**, 140501(R) (2011)

Structure-induced coexistence of ferromagnetic and superconducting states of single-phase Bi_3Ni seen via magnetization and resistance measurements

T. Herrmannsdörfer,[1] R. Skrotzki,[1,2] J. Wosnitza,[1] D. Köhler,[2] R. Boldt,[2,*] and M. Ruck[2]

[1]*Dresden High Magnetic Field Laboratory (HLD), Helmholtz-Zentrum Dresden Rossendorf, D-01328 Dresden, Germany*

[2]*Department of Chemistry and Food Chemistry, TU Dresden, D-01062 Dresden, Germany*

(Received 9 May 2010; revised manuscript received 31 January 2011; published 5 April 2011)

We demonstrate the coexistence of superconductivity and ferromagnetism in Bi_3Ni nanostructures that have been prepared by making use of novel chemical-reaction paths. We have characterized their magnetic and superconducting properties by means of magnetometry and electrical-transport measurements. Other than in bulk geometry, submicrometer-sized particles and quasi-one-dimensional nanoscaled strains of single-phase Bi_3Ni undergo ferromagnetic order. Superconductivity in confined Bi_3Ni emerges in the ferromagnetically ordered phase and is stable up to remarkably high magnetic fields. Uniquely, ferromagnetic hysteresis at zero resistance is observed in nanostructured Bi_3Ni.

DOI: 10.1103/PhysRevB.83.140501 PACS number(s): 74.25.Ha, 74.70.Ad, 74.78.Na, 75.75.Cd

Superconductivity and ferromagnetism, two fundamental ground states of condensed matter, are observed to be highly competitive in almost any material. Predominant ferromagnetic exchange interactions destroy superconductivity by creating a reentrant phase transition as observed in $ErRh_4B_4$, $HoMo_6S_8$, and related materials.[1] Only very few compounds have been identified so far that show a coexistence of these competing ground states. In $AuIn_2$, a small exchange field of ferromagnetically ordered nuclear magnetic moments is not destroying, although clearly affecting, the Cooper-pair condensate at μK temperatures.[2] In UGe_2,[3] as well as related compounds such as URhGe (Ref. 4) and UCoGe,[5] the coexistence might be even more surprising as superconductivity emerges at temperatures where ferromagnetism is already established. The itinerant character of 5*f* electrons in UGe_2 might play a crucial role for the coexistence.[3] This is in striking contrast to any other material, in particular, to metallic elements. Among the elements, only few representatives such as Rh (Ref. 6) and granular Pt (Ref. 7) reveal a coexistence of Cooper pairs in balance with weak magnetic correlations that do not establish a magnetically ordered ground state. Even materials where superconductivity coexists with a magnetic ground state that solely exhibits a weak ferromagnetic component of its magnetization, e.g., Y_9Co_7,[8] the magnetic high-temperature superconductor $RuSr_2GdCu_2O_8$ (Ref. 9) or $ErNi_2B_2C$ where weak ferromagnetic ordering arises at twin boundaries of antiferromagnetic domains,[10] are very rare. The study of electronically confined intermetallics, however, may bear the chance to find much more systems that exhibit coexistence phenomena of superconductivity and magnetism. As shown here for the material Bi_3Ni, structural confinement creates ferromagnetic order in a material that is nonmagnetic in bulk topology. At lowest temperatures, these size-dependent magnetic correlations eventually compete and surprisingly coexist with superconductivity.

Superconductivity in the intermetallic compound Bi_3Ni had been reported many years ago.[11] Although containing the transition metal Ni, it is known to be "nonmagnetic."[12] In fact, the Ni 3*d*-electron band is filled, and bulk Bi_3Ni exhibits temperature-independent Pauli paramagnetism. For this reason, an interplay of superconductivity and magnetism could have only been studied by gradually replacing the 3*d*-electron element by magnetic 4*f*-electron lanthanide ions, as has been performed for the isostructural compound $Bi_3Sr_{1-x}Eu_x$.[13]

The crystal structure of Bi_3Ni is best described as a packing of Bi_3Ni rods [Fig. 1(a)] (Refs. 14–16) where, according to density functional theory calculations, the bonding in the rods is dominated by Bi-Ni and Ni-Ni interactions while Bi-Bi bonds play a minor role.[16] The electron-localization function reveals a separation of delocalized conduction electrons inside the prism rods and largely localized valence electrons between them. Overall, the bonding between the intermetallic rods is clearly weaker than inside them, leading to a preservation of this structural fragment in the halogenides of Bi_3Ni,[17–21] e.g., in $Bi_{12}Ni_4I_3 = [Bi_3Ni]_4I_3$,[17] where Bi_3Ni rods are separated by insulating iodide anions [Fig. 1(b)]. For the synthesis of nanostructured Bi_3Ni, we have treated $Bi_{12}Ni_4I_3$ with *n*-butyllithium at room temperature in order to remove the iodine. This reductive etching of $Bi_{12}Ni_4I_3$ resulted in a pseudomorphosis of the crystalline material into a three-dimensional (3D) assembly of nanofibers of Bi_3Ni [Fig. 1(c)]. We may assume that the spatial arrangement of the one-dimensional (1D) Bi_3Ni rods present in the iodide $Bi_{12}Ni_4I_3$ is preserved owing to the mild conditions, because the reformation of the rod packing of the bulk phase is kinetically hindered. The x-ray powder diffraction pattern of nanostructured Bi_3Ni only shows broad humps that correspond to typical interatomic distances in Bi_3Ni [Fig. 1(d)].[16] In other words, similar to a nematic liquid crystal, macroscopic supercrystals of incoherently but parallel packed nanofibers with individual diameters below 5 nm were obtained. Only upon annealing the nanostructured Bi_3Ni at ~700 K, the 3D order of the crystalline bulk material is regained. The recrystallization was used for the preparation of bulk Bi_3Ni (bulk powder with grain diameters $\gtrsim 20\ \mu$m) as a reference material. The precursor compound $Bi_{12}Ni_4I_3$ shows a temperature-independent diamagnetic susceptibility of $-30\ \mu$emu/g. Thus, hypothetical traces of $Bi_{12}Ni_4I_3$ would not bias the magnetic moments of the Bi_3Ni samples. However, $Bi_{12}Ni_4I_3$ is not detectible in the x-ray diffraction pattern of the nanostructured Bi_3Ni sample [Fig. 1(d)] and no iodine has been found in the chemical analysis by energy-dispersive x-ray spectroscopy. In order to allow for the investigation of the

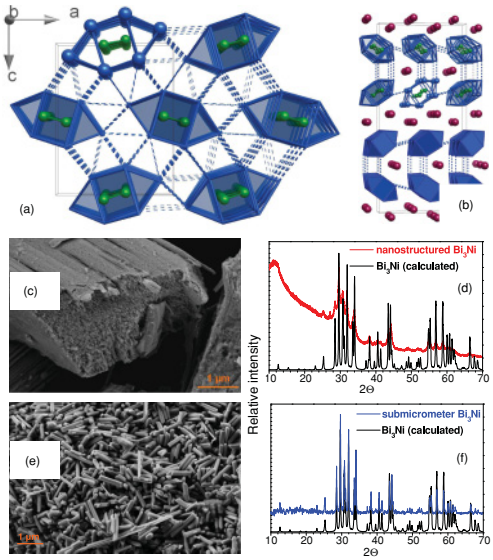

FIG. 1. (Color online) Crystal structure of bulk and submicrometer Bi_3Ni (Bi blue, Ni green) (a) as well of the metal–insulator-hybrid $Bi_{12}Ni_4I_3$ (b) used as a reagent for the synthesis of nanostructured Bi_3Ni, where infinite Bi_3Ni rods are separated by iodide ions (red). Electron micrographs of nanostructured (c) and submicrometer Bi_3Ni (e) are displayed. Their broadened x-ray powder-diffraction patterns (d), (f) are compared to a calculation for bulk material.

properties of Bi_3Ni at a length scale intermediate between bulk powder and the nanostructured material, a microwave-assisted low-temperature synthesis starting from metal acetates was developed. Under a variation of external parameters, phase-pure crystalline Bi_3Ni particles with a uniform size and shape ($l \approx 600$ nm, $d \approx 200$ nm) were obtained [Fig. 1(e)]. This material is subsequently denoted as submicrometer Bi_3Ni.

For the characterization of the superconducting and magnetic sample properties, magnetization has been measured by means of superconducting quantum interference device (SQUID) and vibrating-sample magnetometry at temperatures between 1.8 and 300 K. Measurements of the electrical transport properties were performed by means of an ac four-terminal contact technique. A commercial cryostat equipped with a superconducting 14-T magnet and a ^{3}He refrigerator were used for measurements in the temperature range between 0.35 and 300 K.

Bi_3Ni in bulk, submicrometer, as well as nanostructured topology exhibits type-II superconductivity. In bulk Bi_3Ni powder prepared for this work, a superconducting transition temperature, $T_c = 4.06$ K [see Fig. 2(a)], has been observed in accordance with literature.[11] We have identified a Meißner phase up to a field of $\mu_0 H_{c1} \approx 15$ mT, followed by a Shubnikov phase that extends up to approximately $\mu_0 H_{c2} = 0.4$ T (not shown). As compared to bulk material, type-II superconductivity escorted by widened transitions with an elevated onset temperature (see also Fig. 4) but reduced 50% of its normal-state resistance temperature also exists in size-confined Bi_3Ni. In submicrometer as well as in nanostructured topology, the diamagnetic field expulsion in the superconducting state of Bi_3Ni appears to be more complex. A low-field study ($\mu_0 H = 5$ mT), presented in Fig. 2(a), evidences a distinct irreversibility depending on the field and temperature prehistory. The

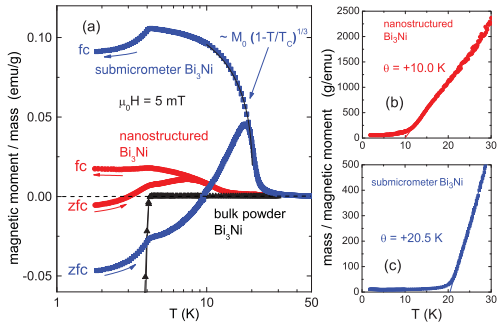

FIG. 2. (Color online) (a) Magnetic moment of nanostructured (red), submicrometer (blue), and bulk Bi_3Ni (black) as function of temperature in $\mu_0 H = 5$ mT. Positive Weiss temperatures (b), (c) and typical power-law dependences of the magnetic moment indicate ferromagnetic spin-spin interactions in the ordered state of confined Bi_3Ni. Superconductivity and magnetic order are attended by a zero-field-cooled (ZFC) and field-cooled (FC) irreversibility in confined Bi_3Ni (a).

application of a magnetic field after zero-field cooling (ZFC) leads to larger field expulsion than in the case of cooling the materials in magnetic fields [field cooled (FC)]. Most remarkably, the magnetic moment of nanostructured and submicrometer Bi_3Ni shows clear indications for the occurrence of magnetic order while bulk Bi_3Ni is nonmagnetic. ZFC in the superconducting state, application of a magnetic field, and subsequent warming up to above T_c leads to a peak behavior of the magnetization at the magnetic ordering temperature owing to temperature dependence of diamagnetic susceptibility in the superconducting as well as an orientation of magnetic domains in the magnetically ordered regime of confined Bi_3Ni [see Fig. 2(a)]. At elevated temperatures, the magnetic moments of both confined Bi_3Ni structures follow a Curie-Weiss law with positive Weiss temperatures, $\Theta = +10$ K [nanostructured, see Fig. 2(b)] and $\Theta = +20.5$ K [submicrometer, see Fig. 2(c)]. At $T \lesssim \Theta$, in the case of FC, the magnetic moment increases as $m = m_0(1 - T/T_{\mathrm{Curie}})^{1/3}$, clearly indicating the formation of a spontaneous magnetization below the Curie temperature where $T_{\mathrm{Curie}} \sim \Theta$ [Fig. 2(a)].[22] We note that a recent study[23] of bulk samples containing 96.8% Bi_3Ni and other phases reports magnetization data with a small contribution (~1% of the diamagnetic moment in the superconducting state) that is partially attributed to a ferromagnetic component. However, we did not observe a ferromagnetic contribution in our bulk Bi_3Ni samples.

Apparently, the origin of ferromagnetic spin-spin couplings in Bi_3Ni is a direct result of the reduction of the sample size in less than 3D. The size confinement leads to a high surface fraction, which modifies the electronic band structure, e.g., owing to surface-tension effects. As compared to bulk Bi_3Ni, the Bloch states of quasiparticles in confined Bi_3Ni are modified and electron-electron interactions might be affected by additional scattering mechanisms, as discussed for Pt.[24] A hypothetical partial depletion of the Ni-3*d* conduction electron band would give rise to the formation of magnetic moments and their correlations in submicrometer and nanostructured Bi_3Ni. For nanostructured Bi_3Ni, the transformation from a 3D into a 1D structure with essentially reduced interaction between Bi_3Ni strands may further affect the band structure.

For deeper insight into the superconducting and magnetic properties as well as their mutual interplay, we have investigated the magnetic properties of nanostructured and submicrometer Bi_3Ni at higher magnetic fields (Fig.3). In these confined Bi_3Ni structures, ferromagnetic hysteresis modified by superconducting diamagnetic screening emerges below T_c [Fig. 3(a)]. Most interestingly, ferromagnetic hysteresis and superconductivity appear in the same sample volume. This can clearly be seen for submicrometer Bi_3Ni by comparing magnetization data taken at $|\mu_0 H| \leqslant 60$ mT below and above T_c. While a ferromagnetic initial magnetization curve is observed for $T \gtrsim T_c$ [see magnetization data for $T = 5$ K and 15 K in Fig. 3(c)], a Meißner phase with diamagnetic field screening modified by the London penetration depth emerges at temperatures below without any appearance of magnetic hysteresis effects at $|\mu_0 H| \leqslant 60$ mT [see data for $T = 1.8$ K in Figs. 3(a) and 3(c)]. The entire suppression of magnetic hysteresis in the Meißner phase is an outstanding feature as the field penetration into the grains that have a size comparable to the London penetration depth (∼200 nm) is evident. In fact, a diamagnetic volume susceptibility of submicrometer Bi_3Ni of ~ -0.06 (compared to -1 for bulk material) observed at $T = 1.8$ K and $|\mu_0 H| \leqslant 60$ mT matches well with a calculation that considers field penetration into submicrometer-sized crystallites on a length scale of the London penetration depth, according to Ref. 25. At fields beyond 60 mT, a ferromagnetic hysteresis loop emerges for submicrometer Bi_3Ni that is superimposed and essentially broadened by the superconducting state at $T \leqslant T_c$. To the best of our knowledge, such a definitive appearance of superconductivity and ferromagnetic characteristics has never been observed before in a single-phase material. The mutual interplay with superconductivity enlarges the coercive field almost by a factor of 4 to 300 mT [Fig. 3(c)]. This finding promotes speculations that ferromagnetism and superconductivity correlate and mutually consolidate each other. At high magnetic fields, the magnetizations of submicrometer and nanostructured Bi_3Ni clearly differ. In nanostructured

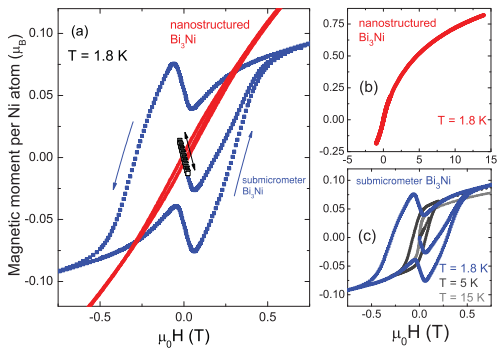

FIG. 3. (Color online) Magnetic moment per Ni atom of nanostructured (red) and submicrometer Bi_3Ni (blue) as function of $\mu_0 H$ at $T = 1.8$ K (a). For nanostructured Bi_3Ni, the magnetic moment is also displayed at fields up to 14 T (b). For submicrometer material, the evolution of the magnetic hysteresis loop with temperature and its interference with superconductivity at $T \leqslant T_c$ is shown (c). A fully reversible Meißner state is present in submicrometer Bi_3Ni at $|\mu_0 H| \leqslant 60$ mT (black open squares and double arrow) at $T = 1.8$ K after ZFC (a).

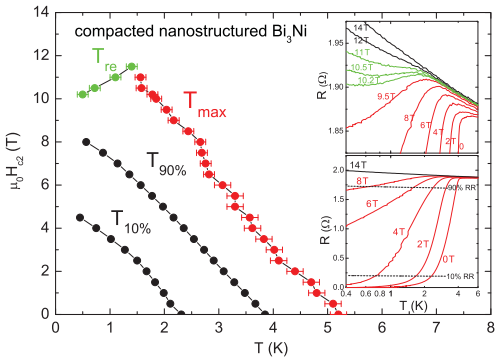

FIG. 4. (Color online) Superconducting field-temperature phase diagram deduced from measurements of the electrical resistance (insets) of compacted ($P = 5$ kbar) nanostructured Bi_3Ni. The horizontal lines mark the 90% and 10% value (lower inset) of the normal-state resistance. The temperatures where $R(T,H)$ decays below a maximum resistance (at T_{max}) and where a reincrease sets in (at T_{re}) are also used as indicators for the upper limit of the onset of Cooper pairing (upper inset).

Bi_3Ni, coercive field, remnant magnetization, and diamagnetic screening are reduced, while magnetic moment and saturation field are clearly increased [Fig. 3(b)]. Whereas the magnetization of submicrometer-sized material saturates at $|\mu_0 H| \approx 1$ T, with a small magnetic moment of $0.1\mu_B$ per Ni atom, there is no indication of saturation in the nanostructured representative up to 14 T where $0.8\mu_B$ per Ni atom is found [Fig. 3(b)]. We started to investigate the magnetic properties of nanostructured Bi_3Ni further in pulsed magnetic fields up to 60 T where a magnetic moment of $\sim 1.5\mu_B$ per Ni atom is measured. Even up to these fields, a full orientation of all Ni moments has not yet been realized and further measurements to the more challenging field range above 60 T are required. Quite obviously, the magnetic moment in randomly oriented particles consisting of nanostructured 1D strands of molecular diameter are much harder to polarize, presumably owing to a strong exchange and shape anisotropy. Possibly, also the tighter hysteresis loop and the smaller Curie temperature of nanostructured as compared to submicrometer Bi_3Ni [see Fig. 3(a)] originates from that quasi-1D anisotropy.

For a proper determination of the superconducting upper critical field, we have also performed measurements of the electrical resistivity of nanostructured Bi_3Ni that has been moderately compacted to a granular sponge consisting of nanoscaled fragments. Data have been taken at $0.4\text{ K} \leqslant T \leqslant 300$ K and fields up to 14 T (see insets in Fig. 4). An H-T phase diagram has been constructed by analyzing the $R(T,H)$ curves for characteristic values, $R(T,H)/R_{max}(H) = 10\%$ and 90% (see the main frame of Fig. 4). In particular, we focus on such temperatures, T_{max}, where $R(T,H)$ shows first deviations from normal-state behavior and where Cooper pairing emerges in the high-field vortex-liquid state (see, e.g., Ref. 26) of nanostructured Bi_3Ni. Although the onset of superconductivity of nanostructured Bi_3Ni is just 5.2 K, its upper critical magnetic field reaches approximately $\mu_0 H_{c2} = 11$ T (Fig.4). At $\mu_0 H > 10$ T, we observe an indication for the existence of a low-temperature reentrant phase in a narrow region of field and temperature indicated by a reincrease of the electrical resistance (Fig.4). The critical field is distinctly

raised owing to the reduced length scale, $d \ll \xi$, where d is the diameter of Bi_3Ni strands, $\xi = (\phi_0/2\pi\mu_0 H_{c2})^{1/2}$ is the superconducting coherence length of bulk Bi_3Ni ($\xi =$ 29 nm for $\mu_0 H_{c2} = 0.4$ T), and $\phi_0 = h/2e$ Wb is the flux quantum. For confined superconductors, the calculation of the critical field is modified to $\mu_0 H_{c2} \approx (\phi_0/2\pi\xi d)$. For $d \approx 1$ nm, this leads to $\mu_0 H_{c2} \approx 11$ T for nanostructured Bi_3Ni, which matches well with the experimental value. The maximum possible critical field to break up Cooper pairs in the singlet state, however, is given by the Zeeman energy. The corresponding theoretical Chandrasekhar-Clogston or Pauli limit,[27] in simple approximation, $\mu_0 H_{P0}/T_c = 1.84$ T/K, is exceeded in nanostructured Bi_3Ni where $\mu_0 H_{P0} = 9.6$ T (Fig. 4). A reason for that might be the influence of a strong spin-orbit scattering, which reduces paramagnetic pair breaking. In that case, the simple approximation of the Pauli-limiting field has to be replaced by $\mu_0 H_P = 1.33(h/3\pi^2 k_B T_c \tau_{SO})^{1/2}\mu_0 H_{P0}$, where τ_{SO} is the spin-orbit scattering time.[28] Also in several other materials, e.g., heavy-fermion systems and organic superconductors, large Maki parameters, $2^{1/2}H_{c2}/H_P$, have been observed.[1,29] In two of them, the organic superconductor κ-(BEDT-TTF)$_2$Cu(NCS)$_2$ and the heavy-fermion system $CeCoIn_5$,[30,31] strong evidence for the occurrence of the so-called Fulde-Ferrell-Larkin-Ovchinnikov superconductivity[32] and for $CeCoIn_5$ a peculiar interplay between superconducting and magnetic ground states have been found recently. In confined nanostructured Bi_3Ni, however, Cooper pairs are even stable in an inhospitable internal magnetic exchange field caused by the formation of ferromagnetic order, i.e., precisely the premise that has been taken by Fulde and Ferrell.[32] The coexistence of superconductivity with ferromagnetic order would most likely be possible in the case of spin-triplet pairing. The absence of an inversion center of the lattice of confined Bi_3Ni would allow for the formation of an antisymmetric spatial component of the electron-wave function and could lead to a significant admixture of a triplet component of the order parameter. However, as the lattice of bulk Bi_3Ni is centrosymmetric, the question remains as to whether the loss of structural long-range order at the surface of confined nanostructures could induce antisymmetry of the charge carrier wave function. The results, demonstrated in Fig. 4, in particular, the occurrence of a high-field low-temperature reentrant phase, are a first hint that the onset of the formation of Cooper pairs is linked to the magnetic ground state of confined Bi_3Ni in a rather complex way.

In summary, superconducting and ferromagnetic material properties evidently complement each other in confined Bi_3Ni structures. Superconductivity emerges in the ferromagnetic phase and coexists in the highly spin-polarized ferromagnetic state. With the application of additional experimental techniques, such as nuclear magnetic resonance, deeper insight in the symmetry of the superconducting wave function in k space may be gained. In addition, the preparation and investigation of Bi_3Ni and related compounds also in other sizes ranging from bulk to nanostructured confined geometry will be informative.

We acknowledge the contributions of Y. Skourski to experiments in pulsed magnetic fields. Part of this work was supported by the DFG under contract RU-776/7 and the EU in EuroMagNET II under Contract No. 228043.

*Present address: Leibniz Institute of Polymer Research, D-01069 Dresden, Germany

[1] M. Maple *et al.*, in *Superconductivity*, edited by K. Bennemann and J. Ketterson (Springer, Berlin, 2008), Vol. 1, p. 639–762.
[2] S. Rehmann, T. Herrmannsdörfer, and F. Pobell, Phys. Rev. Lett. **78**, 1122 (1997).
[3] S. S. Saxena *et al.*, Nature (London) **406**, 587 (2000).
[4] D. Aoki *et al.*, Nature (London) **413**, 613 (2001); F. Levy *et al.*, Nat. Phys. **3**, 460 (2007).
[5] N. T. Huy, A. Gasparini, D. E. de Nijs, Y. Huang, J. C. P. Klaasse, T. Gortenmulder, A. de Visser, A. Hamann, T. Gorlach, and H. v. Löhneysen, Phys. Rev. Lett. **99**, 067006 (2007).
[6] Ch. Buchal, F. Pobell, R. M. Mueller, M. Kubota, and J. R. Owers-Bradley, Phys. Rev. Lett. **50**, 64 (1983).
[7] R. König, A. Schindler, and T. Herrmannsdörfer, Phys. Rev. Lett. **82**, 4528 (1999).
[8] A. Kolodziejczyk, IEEE/CSC & ESAS European Superconductivity News Forum, No. 1, 1 (2007).
[9] B. Bohnenbuck *et al.*, Phys. Rev. Lett. **102**, 037205 (2009) and references cited therein.
[10] I. S. Veschunov, L. Y. Vinnikov, S. L. Budko, and P. C. Canfield, Phys. Rev. B **76**, 174506 (2007).
[11] N. Alekseevskii, Zh. Eksp. Teor. Fiz. **18**, 101 (1948).
[12] G. Voss, Anorg. Chem. **57**, 34 (1908).
[13] B. Kempf, B. Elschner, P. Spitzli, and O. Fischer, Phys. Rev. B **17**, 2163 (1978).
[14] V. Glagoleva and G. Zhdanov, Zh. Eksp. Teor. Fiz. SSSR **26**, 337 (1964).
[15] H. Fjellvag *et al.*, Less-Common Met. **128**, 177 (1987).
[16] M. Ruck and T. Söhnel, Z. Naturforsch. **61b**, 785 (2006).
[17] M. Ruck, Z. Anorg. Allg. Chem. **623**, 243 (1997).
[18] M. Ruck, Z. Anorg. Allg. Chem. **625**, 453 (1999).
[19] B. Wahl *et al.*, Anorg. Allg. Chem. **631**, 457 (2005).
[20] B. Wahl and M. Ruck, Acta Crystallogr. B **65**, 593 (2009).
[21] M. Ruck, Angew. Chem. **113**, 1222 (2001); Angew. Chem. Int. Ed. **40**, 1182 (2001).
[22] L. de Jongh and A. Miedema, Adv. Phys. **50**, 947 (2001).
[23] E. Martinez Piñeiro *et al.*, e-print arXiv:1101.2226.
[24] D. Fay and J. Appel, Phys. Rev. Lett. **89**, 127001 (2002).
[25] D. Shoenberg, Proc. R. Soc. London, Ser. A **175**, 49 (1940).
[26] B. Halperin *et al.*, *BCS: 50 Years*, edited by L. Cooper and D. Feldman (World Scientific, New Jersey, 2010), pp. 185–226.
[27] A. Clogston, Phys. Rev. Lett. **9**, 266 (1962).
[28] K. Maki, Phys. Rev. **148**, 362 (1966).
[29] O. Fischer, *Ferromagnetic Materials*, edited by K. Buschow and E. Wohlfahrt (Elsevier, Amsterdam, 1990), Vol. 5, p. 465.
[30] R. Lortz, Y. Wang, A. Demuer, P. H. M. Böttger, B. Bergk, G. Zwicknagl, Y. Nakazawa, and J. Wosnitza, Phys. Rev. Lett. **99**, 187002 (2007); G. Zwicknagl and J. Wosnitza, *BCS: 50 Years*, edited by L. Cooper and D. Feldman (World Scientific, New Jersey, 2010), pp. 337–371.
[31] M. Kenzelmann *et al.*, Science **321**, 1652 (2008).
[32] P. Fulde and R. Ferrell, Phys. Rev. **135**, A550 (1964).